
Article:
Qiu, L, Wu, J, Du, W et al. (5 more authors) (2021) Response of soil bacterial communities to sulfadiazine present in manure: Protection and adaptation mechanisms of extracellular polymeric substances. Journal of Hazardous Materials, 408. 124887. ISSN 0304-3894

https://doi.org/10.1016/j.jhazmat.2020.124887

Response of Soil Bacterial Communities to Sulfadiazine Present in Manure: Protection and Adaptation Mechanisms of Extracellular Polymeric Substances

Linlin Qiu,[a] *Jingjing Wu,*[a] *Wenchao Du,*[b] *Muhammad Nafees,*[a] *Ying Yin,*[a] *Rong Ji,*[a] *Steven A. Banwart,*[c,d] *Hongyan Guo*[a,]*

[a] State Key Laboratory of Pollution Control and Resource Reuse, School of the Environment, Nanjing University, Nanjing, Jiangsu 210023, China

[b] School of Environment, Nanjing Normal University, Nanjing 210023, China

[c] School of Earth and Environment, University of Leeds, Leeds, LS2 9JT, UK

[d] Global Food and Environment Institute, University of Leeds, Leeds, LS2 9JT, UK

* Corresponding author. Tel.: +86-25-89680263; Fax: +86-25-89680263.

E-mail address: hyguo@nju.edu.cn (H. Guo).

Abstract

Extracellular polymeric substances (EPS) play a dominant role in protective biofilms. However, studies exploring the underlying protective mechanism of EPS have mainly focused on activated sludge, whereas their positive roles in protecting soil microbes from environmental stress have not been elucidated. In this study, we revealed the response of soil bacterial communities to various dosages of sulfadiazine (SDZ) present in manure, with a special emphasis on the role of EPS. Sequencing analysis showed that the bacterial community demonstrated stronger symbiotic relationships and weaker competitive interaction patterns to cope with disturbances induced by SDZ. EPS was mainly composed of tyrosine-like and tryptophan-like substances, and moreover, carboxyl, hydroxyl and ether groups were the main functional groups. An adaptation mechanism, namely the enhanced secretion of tryptophan-like substances, could help alleviate the SDZ stress effectively in the biofilms occurring in soil that experienced long-term manure application. Furthermore, the existence of EPS weakened the accumulation of antibiotic resistance genes (ARGs) in soil. Our results for the first time systematically uncover the joint action of biofilm tolerance and ARGs in resisting SDZ stress, which enhances understanding of the protective role of EPS and the underlying mechanisms governing biofilm functions in soil environments.

Keywords: EPS, antibiotic resistance, sulfonamides

1. Introduction

Sulfonamides with low price and high efficiency of restraining the growth of micro-organisms have seen extensive usage since the 1940s in worldwide animal husbandry for therapeutic and prophylactic use to enable intensification of food animal production (Baran et al., 2011). The poor assimilation and incomplete metabolism of sulfonamides that occurs in the gut of animals has led to a large proportion excreted unchanged or modified to other bioactive metabolites in faeces and urine (Schauss et al., 2009; Jechalke et al., 2014). Manure application could accelerate the development and epidemic spread of antibiotic resistance genes (ARGs) not only because the co-excretion of parent substance and metabolites can provide selective pressure, but because excreta is an important reservoir of antibiotic resistance bacteria (ARB) and ARGs (Jechalke et al., 2014; Udikovic-Kolic et al., 2014). The increasing prevalence of ARGs will pose global threats to public health, and even result in the emergence of multidrug-resistant superbugs and is regarded as one of the worst-case scenarios for emerging global risks to public health and medical treatments (Udikovic-Kolic et al., 2014; Zhu et al., 2013).

The bloom of ARGs in the natural environment results from three principle mechanisms which exist in combination, namely the proliferation of ARB due to selective pressures, genetic mutation and recombination, along with the horizontal gene transfer of ARGs (Berendonk et al., 2015). Mobile genetic elements (MGEs) loaded with ARGs shuttles between bacterial hosts resulting in the dissemination of antibiotic resistance (Gootz, 2010, Bellanger et al., 2014). Molecular mechanisms of antibiotic

resistance mainly fall into two groups: those that impede antibiotic access to target receptors through reduction of cell wall permeability to slow uptake and increasing efflux of active compounds out of the cell; those that hinder antibiotic binding to target receptors through inactivation of the antibiotic and modification of target receptors (Blair et al., 2015). To date, research on antibiotic resistance in soil environments mainly focuses on the role of ARGs (Liang et al., 2017; Hall et al., 2020; Wang et al., 2018a; Muurinen et al., 2017; Xie et al., 2016). In fact, microbes within a biofilm state could become less susceptible to antibiotic compounds even if lacking ARGs and associated MGEs (Anderl et al., 2000) and noting that numerous soil microorganisms exist within biofilm communities (Redmile-Gordon et al., 2014).

Biofilms are consortia of microbes connected through extracellular polymeric substances (EPS), which take up 80% dry mass of soil biofilms (Chenu, 1993). EPS secreted by microorganisms are mainly present as a complicated matrix predominantly composed of proteins, polysaccharides and extracellular DNA (Redmile-Gordon et al., 2014; Costa et al., 2018). There are a series of mechanisms behind biofilm tolerance and resistance, including transport limitation, sacrificial reaction and nutrient gradient formation (Stewart, 2002). As the principal member in EPS, proteins contain many functional groups and hydrophobic regions that can adsorb a wide range of organic micropollutants including antibiotics (Xu et al., 2013; Wang et al., 2018b; Pi et al., 2019; Wang et al., 2018c; Zhang et al., 2018). Compared to work on the soil environment, research on EPS is more advanced in wastewater treatment plant systems. Studies have reported that EPS in activated sludge served as important reservoirs of

sulfonamides and could alleviate sulfonamides stress effectively (Xu et al., 2013; Wang et al., 2018b; Xu and Sheng, 2020). Proteins played a dominate role in the interaction between EPS and sulfonamides, and moreover, the binding between them was achieved by hydrophobic interactions and functional groups of EPS (Xu et al., 2013; Wang et al., 2018b). However, studies on soil EPS lag behind due to methodological challenges. In fact, only limited research considers the critical roles played by soil EPS in improving water retention, soil aggregate stability and microbial metabolic activity (Adessi et al., 2018; Sher et al., 2020; Wu et al., 2019). Until now, the key role of EPS in antibiotic resistance has not been reported in soil environments. In the light of this important knowledge gap, we hypothesize that soil EPS also play an important part in antibiotic resistance of soil microbes and the generation of EPS can occur independently from the presence of ARGs in soil microorganisms. Hence, there is an urgent need to gain knowledge on the joint action of biofilm tolerance and ARGs in response to antibiotic stress in soil environments.

To gain insight into the role of EPS in biofilm resistance mechanisms in the soil environment, cation exchange resin extraction methods were employed to obtain EPS from soil. Fluorescence excitation−emission matrix (EEM) spectroscopy combined with parallel factor analysis (PARAFAC) were adopted to gain detailed information about EPS composition. Additionally, Fourier transform infrared (FTIR) spectra analysis was carried out to understand the functional groups of EPS. The objectives of this studies were to explore (i) the influence of applying manure spiked with sulfadiazine (SDZ) on soil bacterial community composition and co-occurrence

network; (ii) the protective role of EPS and ARGs in response to SDZ stress; and (iii) the adaptation mechanism exhibited by biofilms resulting from long-term exposure to antibiotics.

2. Materials and methods

2.1 Experimental design and growth condition

Two soil samples with the same mineral parentage were collected separately using spade within 10 cm of surface soil from a bamboo forest and a farmland in Ningbo city, Zhejiang province, China. These two soils are characterized as Regosol according to the classification of the world reference base of soils (WRB). The bamboo forest soil with no history of manure addition while the farmland soil experienced decades of stable manure application. The physicochemical characteristics of the two soil samples are displayed in Table S1 in the Supporting Information (SI). Soil samples were left standing in a ventilated space at room temperature for at least a fortnight to remove moisture and then passed through 2 mm sieves. Bench-scale pot experiments were designed using manure spiked with different doses of SDZ to mimic a gradient of contamination, namely clean (0 mg kg^{-1}), low (5 mg kg^{-1}), moderate (10 mg kg^{-1}) and high (100 mg kg^{-1}) contaminated manure. Low dosing in our study corresponded to about 10 fold of an average environmentally relevant concentration (Deng et al., 2018). These four mixtures of manure and SDZ were incorporated individually with the two soil samples to form 8 treatments with four replicates each and 32 pots in total. Each pot was filled with 200 g soil, 8 g manure and some water to maintain at 60% of the soil's water-holding capacity. Ten seeds of pak choi (Brassica rapa subsp. chinensis)

were scattered in the surface soil and thinned out during germination. All of the pots were placed randomly side by side in the greenhouse (temperature of 25 °C, relative humidity of 60-70% and 14-h photoperiod). During the growth of pak choi, equal amount of tap water was added to every pot approximately every two days. The pak choi plants were harvested on the 40th day after planting. Simultaneously, soil samples were collected after harvesting the pakchoi plants for further analysis.

2.2 Extraction protocol and characterization of EPS

The method adopted to extract EPS was cation exchange resin extraction as described by Redmile-Gordon et al. (2014), which is described in detail in Text S1. The concentration of dissolved organic carbon (DOC) was used as an indicator of EPS quantity. The EPS extract was passed through 0.45 μm polytetrafluoroethylene membranes and then determined using a TOC analyzer (vario TOC, Elementar, Germany). The composition of EPS was characterized by Fluorescence excitation−emission matrix (EEM) spectroscopy and Fourier transform infrared (FTIR) spectra respectively. To avoid the inner filtering effects, EPS samples were diluted with ultra-pure water to ensure that the DOC concentration was lower than 10 mg L^{-1}. The fluorescence EEM spectra was recorded with excitation ranges between 220-490 nm and emission ranges between 250-550 nm using a F-7000 fluorescence spectrometer (Hitachi High Technologies, Japan). The EEMs were determined by subtracting the ultra-pure water signal first and then removing the Rayleigh and Raman scatter signals. Subsequently PARAFAC was conducted using MATLAB 2019a with a DOMFluor toolbox as described by Stedmon and Rasmus (2008). Split half analysis, residual

analysis and sum of squared error analysis were carried out during the process of determining the number of components.

The lyophilized EPS extract and infrared grade KBr were mixed with a ratio of 1:100 and homogenized in an agate grinder. About 100 mg of the mixture was analyzed by a FTIR spectrometer (NEXUS870, NICOLET, USA) with a spectral range of 4000-400 cm^{-1}, 32 scans and a spectral resolution of 4 cm^{-1}.

2.3 Two-Dimensional (2D) FTIR Correlation Spectroscopy

To get the structural variation information of EPS, 2D correlation spectra were conducted following the method of Noda and Ozaki (2004). In this study, SDZ concentration was considered as an external perturbation. Then synchronous and asynchronous correlation spectroscopy was generated using the 2Dshige software (Kwansei-Gakuin University, Japan). The region from 1400 to 800 cm^{-1} was focused and analyzed in detail here, because the major bands were included in this zone. Spectral coordinates, intensities and signs of correlation peaks appearing on 2D spectra could be interpreted according to well-established principles (Noda and Ozaki, 2004; Noda, 2012).

2.4 Sequencing and bioinformatics analysis

Microbial DNA was extracted from lyophilized soil for qPCR and sequencing following the protocol of MoBio DNeasy Powersoil Kit (MoBio, Carlsbad, CA, USA). The modified primer pair 341F/518R was used to amplify the V3 region of 16S rRNA (Klindworth et al., 2012). Unique 12-nt barcode oligonucleotides were connected to the

5′-ends of the forward primer to distinguish different soil microbial DNA in the mixed pool. The reaction mixtures and the amplification protocol followed a previous study (Li et al., 2018). The size and quality of PCR products were checked through visualizing on a 2% agarose gel. The checked products were purified using the E-Z 96 Cycle Pure Kit (Omega, U.S.A.). Qubit dsDNA HS Assay Kits (Invitrogen, U.S.A.) were used to determine the concentration of clean PCR products. Then, products were pooled in equimolar concentrations and were subjected to library preparation followed the procedure of Ion Xpress Plus Fragment Library Kit (Thermo Fisher Scientific, U.S.A.). Afterwards, all of the products were diluted to 100 pM. The diluted products were subjected to cluster generation and sequenced in the Ion Proton sequencer (Life Technologies, U.S.A.). QIIME2 (v.2019.7) was employed to analyze raw sequence data through the following process: demultiplex, quality control, and taxonomy classification (Klindworth et al., 2012). Sequence quality control and the generation of amplicon sequence variants (ASVs) were performed using the DADA2 method (Callahan et al., 2016). After that, a feature table was produced. Silva database was choose to conduct the taxonomy annotation for each sequence (Quast et al., 2012)

2.5 ARGs abundance analysis

The qPCR was conducted using an ABI QuantStudio 12K Real-Time PCR System (Applied Biosystems, USA). The primer sequences are demonstrated in Table S2. Four standard plasmids including *sul1*, *sul2*, *intI1*and 16S rRNA were employed to generate calibration curves. The protocol of making standard plasmids has been describe elsewhere (Chen et al., 2018). A 20 μL qPCR mixture was made up of 2 × SYBR Green

Premix Ex Taq (Takara, 5 μL), forward/reverse primers (10 μM, 0.8 μL), DNA template (2 μL), ddH_2O (3 μL) and ROX (0.2 μL). The amplification condition was as follows: 95 ℃ for 5 min followed by 35 cycles of 95 ℃ for 5 s, annealing at 55 ℃ (16S rRNA, *sul1* and *sul2*) or 63 ℃ (*intI1*) for 30 s and 72 ℃ for 30 s. Triplicate reactions were carried out for each sample to check the reproducibility and weaken the potential bias of PCR.

2.6 Statistical analysis

Statistical comparisons of EPS quantity, the abundance of ARGs and Shannon index were examined by one-way analysis of variance (ANOVA) with Fisher's least significant difference (LSD) tests in SPSS 26.0 software (SPSS, Chicago, IL, USA). Principal coordinate analysis (PCoA) was conducted based on the Bray-Curtis distances to evaluate the influence of SDZ on bacterial community composition (Anderson and Willis, 2003). Moreover, Permutational multivariate analysis of variance (PERMANOVA) was employed to determine effect size and significances on beta-diversity using "Adonis" function in "Vegan" package of R project (Anderson, 2001). An on-line linear discriminant analysis of effect size (LefSe) analysis was carried out at http://huttenhower.sph.harvard.edu/galaxy to detect markedly different species for different groups (Segata et al., 2011). The alpha value for the factorial Kruskal-Wallis test among treatments was 0.05 and the threshold on the logarithmic LDA score for discriminative features was 2.0. Samples from bamboo forest soil and farmland soil under SDZ exposure (Low, Moderate and High) were used to perform network analysis to investigate variations in interactions between microbes caused by SDZ exposure.

The co-occurrence network was constructed by calculating a similarity matrix based on the Spearman correlation coefficient. The correlation threshold was above 0.8 and the *p* value was below 0.01. To identify highly associated nodes, Molecular Complex Detection (MCODE) was employed on the Cytoscape platform (Bader and Hogue, 2003). Finally, Gephi software was used to achieve network visualization (Bastian and Jacomy, 2009).

3. Results and discussion

3.1 Shift in bacterial community and co-occurrence networks in the presence of SDZ

Natural soil from bamboo forest was compared with farmland soil receiving long-term manure application to explore the acute and chronic response of the soil bacterial communities with the emergence of SDZ as a pollutant of concern. A total of 1,816,492 high-quality bacterial sequences were detected through the Ion Torrent sequencing platform. For both soils, the alpha-diversity of the bacterial community measured by the Shannon index was significantly increased with high concentrations SDZ ($p < 0.05$, Figure 1a). To detect if there existed phylogenetic relations between the soil bacterial communities, a PCoA was conducted based on the Bray-Curtis metric distance. PCoA demonstrated a clear separation between the bamboo forest and farmland soils (Figure 1b). Furthermore, a PERMANOVA test indicated that the bacterial community was noticeable influenced by the soil type (11.4%, $p = 0.001$), which also demonstrated the pronounced differences in bacterial community between two soils.

To extend the understanding of bacterial community changes, we next sought to

examine the difference in the soil microbiome composition at taxonomic level (Figure 1c). The general landscape of bacterial taxa showed that all samples exhibited similar taxonomic composition and that the dominant phyla were *Proteobacteria*, *Actinobacteria*, *Acidobacteria*, *Gemmatimonadetes*, *Planctomycetes*, *Bacteroidetes*, *Chloroflexi* and *Firmicutes*. *Proteobacteria* and *Actinobacteria* were the most abundant phyla, accounting for 28.62–32.33% and 21.90–34.57% in bamboo forest and farmland soils respectively. For the bacterial community of the bamboo forest soil, *Actinobacteria* was enriched at low concentrations of SDZ, while *Acidobacteria* and *Gemmatimonadetes* were overrepresented at moderate SDZ concentrations, and moreover *Chloroflexi* and *Nitrospirae* were enriched at high SDZ concentrations. With regard to farmland soil, the low concentrations shared an extremely similar bacteria community composition with the control soil, while the bacterial communities exposed to moderate SDZ concentrations demonstrated a community composition that was similar to that for high SDZ exposure. In general, the relative abundance of *Proteobacteria*, *Acidobacteria*, *Gemmatimonadetes* and *Nitrospirae* increased in the presence of moderate and high concentrations of SDZ, while there was a noticeable decline in *Actinobacteria* and *Firmicutes* abundance. In fact, *Actinobacteria* is composed of various crucial microbes in soil playing important ecological roles including recycling of substances, degradation of complex organic matter and bioremediation of xenobiotics (Alvarez et al., 2017). Moreover, *Actinobacteria* is a critical component of antibiotic-producing bacteria and some self-resistance mechanisms has been developed by them to survive (D'Costa et al., 2006). In our study,

256 *Actinobacteria* with a significant decline in the relative abundance might lead to a
257 significant change in the overall soil microbial metabolic pattern and self-resistance
258 ability.

259 To further probe the observed differences, LEfSe was carried out to detect marked
260 different species between treatments (Segata et al., 2011). In general, the bamboo forest
261 soil held a greater diversity of marked different species than the farmland soil (Figure
262 S1), indicating that bacteria in farmland soil had stronger tolerance ability to SDZ. For
263 bamboo forest soil, the low concentrations treatment showed a predominance of
264 *Actinobacteria*, *Thermoleophilia* and *Bacilli*, the moderate concentrations treatment
265 exhibited a dominance of *Acidobacteria* and *Gemmatimonadetes*, and the high
266 concentrations treatment was dominated by *Chloroflexia* at the class level (Figure 1d).
267 In contrast, for the bacterial community in the farmland soil, the low concentrations
268 treatment demonstrated an ascendence of *Actinobacteria*, whereas at the moderate SDZ
269 concentrations *Bacteroidetes* (Phylum) and *Gemmatimonadetes* were dominant and
270 with high concentrations conditions showed a predominance of *Acidobacteria* and
271 *Dehalococcoidia* at the class level (Figure 1e).

272 Besides changes in community composition, microbial interactions might also
273 change when responding to external disturbances. To this end, for both soils it was
274 critical to acquire information on co-occurrence networks of soil bacterial communities
275 with SDZ exposure. Results showed that the network of the bacterial community with
276 the addition of SDZ composed of 88 nodes (214 edges) in the bamboo forest soil and
277 96 nodes (185 edges) in the farmland soil (Table S4). The comparable number of nodes

but more edges number in bamboo forest soil indicated that more interactions existed between microbes in bamboo forest soil under SDZ exposure. Through the analysis of the taxonomic feature, we found that the taxa of the bamboo forest soil bacterial network mainly belonged to Bacteroidetes (13.64%), while *Proteobacteria* (15.62%) was the dominant taxa in the farmland soil. Additionally, there were great positive degrees of correlation between bacterial taxa in two soils with the exposure of SDZ (Table S4), which suggested that there was strong symbiotic relationship between microbes with the presence of SDZ. More specifically, the SDZ-treated network of bacterial communities from farmland soil showed the largest positive correlations, over 92%. The bacterial networks were clustered into modules in which the species were assigned functional interdependences and harbored similar ecological niches (Layeghifard et al., 2017). One more modules were identified in the network of bacterial community of bamboo forest soil than that of farmland soil in the presence of SDZ (Figure 2c and 2d), which also suggested that bacteria in bamboo forest showed closer interdependence when coping with SDZ stress.

Overall, changes in the microbiome communities and co-occurrence networks were related to the external SDZ disturbance in both soils. The bacterial community composition of the farmland soil with the long-term manure application exhibited the capability to tolerate low concentrations of SDZ. Moreover, bacterial community of two soils both demonstrated patterns of stronger symbiotic relationships and weaker competitive interactions to survive with the existence of SDZ disturbance.

3.2 Extracellular Interaction shielding by EPS

Many microbes have the capacity to excrete EPS and form protective biofilms to tolerate stresses that emerge in the environment (Stewart, 2002). Variations of the amount of EPS were examined between two soils with the application of manure in the absence and presence of various levels of SDZ (Figure 3a). Compared to the soil from the bamboo forest (208.65 ± 6.15 mg kg^{-1}), the soil from the farmland contained more EPS (300.05 ± 18.51 mg kg^{-1}) with the absence of SDZ in the manure. This result might be related to the fact that manure usually contains some pollutants, such as heavy metals, antibiotics and estrogens (Jechalke et al., 2014; Hanselman et al., 2004), leading to selection of soil microorganisms that can produce more EPS as a survival mechanism. In addition, the farmland soil holds more organic matter mainly due to the long-term application of manure (Table S1), which was conducive to abundant carbon and energy resources for microbial growth and metabolism. When the added manure contaminated high concentrations of SDZ, EPS production increased immensely in both soils. This may indicate the production of microbial EPS as a selection response that confers greater tolerance to SDZ.

Aside from being a physical barrier in the extracellular space, EPS could also provide active sites containing functional groups for interaction with organic contaminants to decrease exposure and environmental stress (Zhang et al., 2018; Sheng et al., 2010). FTIR was carried out to identify the main chemical functional groups present in the EPS. Five main absorbance peaks were observed in the FTIR spectra (Figure 3b), which supplied crucial information about the composition and function of the EPS. The band at 1360 cm^{-1} confirmed the presence of carboxyl (Do et al., 2020). The band around

1160 cm^{-1} corresponds to the stretching vibration of C-O (Yin et al., 2015; Jia et al., 2017; Zhu et al., 2012). The band at about 1075 cm^{-1} was assigned to the ring vibration of C-O-C (Jia et al., 2017; Zhang et al., 2020). The vibration around 950 cm^{-1} is potentially related to the presence of nucleic acids (Jia et al., 2017). The band at approximately 860 cm^{-1} was attributed to the vibration of C-C and C-OH (Jia et al., 2017). Generally, the functional groups composition of the EPS from the bamboo forest soil was similar to that of the EPS from the farmland soil that experienced long-term manure application.

In order to gain more precise information and facilitate the deconvolution of overlapping peaks, 2D-COS analysis was conducted based on the FTIR spectrum. In general, six auto-peaks were observed near 860, 950, 1020, 1110, 1250 and 1360 cm^{-1} in the synchronous map of the EPS from the bamboo forest soil (Figure 3c). Among these peaks, the band at 950 cm^{-1} had the strongest intensity, showing that the O-P-O structure was more susceptible to SDZ concentrations than other groups. All of the cross-peaks were positive, implying that the intensities of these groups proceeded in the same direction with the increase in SDZ concentration. Based on Noda's rule, the intensity variation followed the sequential order C-OH > C-O-C > O-P-O > COOH > C-C (C-OH). In the case of EPS derived from farmland soil, six auto-peaks around 1360, 1200, 1130, 1020, 950 and 860 cm^{-1} appeared in the synchronous map obtained from IR spectrum (Figure 3d). Moreover, the peak centered around 1020 cm^{-1} had the strongest intensity, which implied that C-OH was the most susceptible groups to SDZ addition (Oliveira et al., 2017). The cross-peaks were all positive, also showing that

changes in the intensities of these groups varied in the same direction with increasing SDZ concentration. The same rule could be applied to the synchronous and asynchronous map and it could be concluded that the sequential order of intensity variation was C-O-C > C-OH > COOH > O-P-O > C-C (C-OH).

To eliminate the overlapped absorbance of EEM fluorescence spectra, a PAFAFAC model was employed to provide more reliable and detailed information about EPS composition. Through split half analysis, sum of squared error and residual analysis (Figure S2), all the EEMs (64 samples) could be divided into two protein-like components successfully (Figure 4a). Component 1 representing a tyrosine-like substance with a characteristic peak at Ex/Em (230/295 nm) (Table S5) (Wu et al., 2018; Maqbool et al., 2016; Zhang et al., 2019; Zhang et al., 2016). Component 2 exhibited a fluorescence peak at Ex/Em (270/370 nm) that corresponded well with a tryptophan-like substance observed in previous studies (Table S5) (Wu et al., 2018; Maqbool et al., 2016; Zhang et al., 2019; Zhang et al., 2016; Zhu et al., 2015). In general, the content of C1 in the EPS was approximately double that of C2 (Figure 4b). EPS derived from all the bamboo forest soil shared extremely similar patterns no matter the content of SDZ present in the manure (Figure 4b). Regarding the EPS from the farmland soil, changes in the relative content of the two components became stronger. More specifically, a steady and significant decline could be seen in the proportion of C1 along with the rise of SDZ contained in the manure, decreasing from 65.21 ± 3.00% in the EPS of control soil to 59.64 ± 2.31% in that of soil with high SDZ addition (Figure 4b). In contrast, the content of C2 grew steady from 34.78 ± 3.00% to 40.36 ± 2.31% with

366 increasing concentration of SDZ (Figure 4b).

367 In summary, it appeared that microbes in two soils adopted different strategies to
368 deal with the increasing concentration of SDZ present in the environment. Microbes in
369 the bamboo forest soil seemed to produce more EPS (Figure 3a), and then they could
370 provide more functional groups to adsorb external SDZ to relief stress. Besides
371 increased EPS production and the adsorption of functional groups, microbes in the
372 farmland soil tended to enhance the secretion of tryptophan-like component existed in
373 the EPS to cope with SDZ stress, and this may be related to a mechanism for increased
374 tolerance to SDZ exposure.

375 *3.3 Intercellular Response dominated by ARGs*

376 As SDZ accumulates in the environment, EPS might not hinder antibiotic compound
377 access to the intracellular environment. The transport of SDZ into microbial cells might
378 lead to the excessive production of ARGs. The absolute copy number and relative
379 abundance of class 1 integrons (*intI1*) and two sulfonamide resistance genes (*sul1* and
380 *sul2*) were estimated using the qPCR technology (Figure 5). In general, *intI1* constituted
381 the largest abundance of all targeted ARGs, whereas *sul1* was the least abundant in all
382 samples. Microbes from the farmland soil with the absence of SDZ held higher ARGs
383 abundance than the bamboo forest soil, a result which agreed with previous studies
384 (Muurinen et al., 2017; Tang et al., 2015; Heuer et al., 2011). In terms of the bamboo
385 forest soil, the absolute abundance of these three genes increased immensely with the
386 introduction of moderate to high SDZ concentration in the manure ($p < 0.05$, Figure

387 5a). The moderate concentration of SDZ may cause the significant increase of *sul2*
388 absolute abundance in the farmland soil ($p < 0.05$), while there was only tiny difference
389 in the abundance of *sul1* and *intI1*. It can be concluded that SDZ first enhanced the
390 action of the plasmid in which the *sul2* gene is located (Sköld, 2000). Subsequently,
391 microbes might activate the excessive expression of *sul1* located in the Tn21 type
392 integron to cope with growing SDZ in the environment (Sköld, 2000). For both soils,
393 only the occurrence of high concentrations of SDZ coincided with a significant increase
394 of the relative abundance of *sul1* and *sul2* ($p < 0.05$, Figure 5b). However, there was no
395 noticeable change in the relative abundance of *intI1* between the two soils.

396 *3.4 Protective Mechanisms*

397 The above-mentioned results are consistent with the role of EPS as a microbial first
398 line of defense against external SDZ exposure. Microbes may be shielded by EPS
399 through functional groups that could absorb organic micropollutants. With regard to
400 bamboo forest soil, the acute response of microbes is most likely binding SDZ through
401 the functional group in the EPS, such as carboxyl, hydroxyl, phosphoric and ether group
402 when coping with the low concentration of SDZ (Figure 6a). With the increase in
403 concentration of SDZ, the active sites would be consumed and the EPS would gradually
404 lose its protective action. This may cause antibiotic access to cell and occurrence of
405 ARGs. Even though increased SDZ concentrations may induce microbes to produce
406 more EPS in the extracellular space to reduce the stress of antibiotic exposure, it was
407 still inevitable to induce the bloom of ARGs in cell (Figure 6b). Because of the long-
408 term application of manure, microbes from the farmland soil possessed more EPS and

ARGs in the original soil state (Figure 3a and 5). For this reason, the soil microbes appear to have greater tolerance to SDZ (Figure 6c). When confronted with high concentration of SDZ, the enhanced secretion of tryptophan-like substance occurred and may be part of a mechanism for microbes to ease the chemical stress of SDZ (Figure 6d). Owing to such a possible protective pathway, the bloom of ARGs did not occur, even when exposed to high concentrations of SDZ. On the other hand, a previous study showed that Ca^{2+} could electrostatically bind with the function groups of EPS, consequently, the bridge between plasmids and EPS was established (Hu et al., 2019). This bond could impede the horizontal transfer of plasmid-borne ARGs into recipient cells (Hu et al., 2019). Microbes in farmland soil had a stronger capability of producing EPS, thus, the inhibition of lateral transfer may also be stronger. There are also other biofilm-specific mechanism of resistance and tolerance identified to deal with exogenous disturbance, such as biofilm-specific expression of efflux pumps and protection of oxidative stress (Van et al., 2014). More detailed works about molecular mechanisms of biofilms tolerance and resistance in soil environment are needed in the future.

4. Conclusions

In summary, our study for the first time investigated the joint action of biofilm tolerance and ARGs in resisting SDZ stress in the soil environment. We found that tyrosine-like and tryptophan-like substances were the main components of soil EPS and the main functional groups included carboxyl, hydroxyl and ether groups. EPS likely played a protective role through their functional groups that provided active sites to

adsorb SDZ in the extracellular space, thereby reducing bioavailability. Soil microbial communities that experienced long-term manure applications developed adaptation mechanisms to ease the external SDZ stress. The enhanced secretion of tryptophan-like substances might help avoid the bloom of ARGs in soil environment.

CRediT authorship contribution statement

Linlin Qiu: Writing - Original Draft, Writing - Review & Editing. Jingjing Wu: Investigation, Resources. Wenchao Du: Writing - Review & Editing. Muhammad Nafees: Writing - Review & Editing. Ying Yin: Conceptualization, Writing - Review & Editing. Rong Ji: Conceptualization, Writing - Review & Editing. Steven A. Banwart: Conceptualization, Writing - Review & Editing. Hongyan Guo: Conceptualization, Project administration, Funding acquisition.

Declaration of Competing Interest

The authors declare that they have no known competing financial interests or personal relationships that could have appeared to influence the work reported in this paper.

Acknowledgments

We gratefully acknowledge the financial support of the National Natural Science Foundation of China (no. 41571130061 and 21661132004).

Reference

Adessi, A.; Cruz de Carvalho, R.; De Philippis, R.; Branquinho, C.; Marques da Silva, J., 2018. Microbial extracellular polymeric substances improve water retention in dryland biological soil crusts. Soil Biol. Biochem. 116, 67-69.

https://doi.org/10.1016/j.soilbio.2017.10.002.

Alvarez, A.; Saez, J. M.; Davila Costa, J. S.; Colin, V. L.; Fuentes, M. S.; Cuozzo, S. A.; Benimeli, C. S.; Polti, M. A.; Amoroso, M. J., 2017. Actinobacteria: Current research and perspectives for bioremediation of pesticides and heavy metals. Chemosphere 166, 41-62. https://doi.org/10.1016/j.chemosphere.2016.09.070.

Anderl, J. N.; Franklin, M. J.; Stewart, P. S., 2000. Role of antibiotic penetration limitation in Klebsiella pneumoniae biofilm resistance to ampicillin and ciprofloxacin. Antimicrob. Agents Chemother. 44 (7), 1818-1824. https://doi.org/10.1128/AAC.44.7.1818-1824.2000.

Anderson, M. J., 2001. A new method for non-parametric multivariate analysis of variance. Austral Ecol. 26 (1), 32-46. https://doi.org/10.1046/j.1442-9993.2001.01070.x.

Anderson, M.; Willis, T., 2003. Canonical analysis of principal coordinates: A useful method of constrained ordination for ecology. Ecology 84, 511-525. https://doi.org/10.1890/0012-9658(2003)084[0511:CAOPCA]2.0.CO;2.

Bader, G. D.; Hogue, C. W. V., 2003. An automated method for finding molecular complexes in large protein interaction networks. BMC Bioinf. 4 (1), 2. https://doi.org/10.1186/1471-2105-4-2.

Baran, W.; Adamek, E.; Ziemiańska, J.; Sobczak, A., 2011. Effects of the presence of sulfonamides in the environment and their influence on human health. J. Hazard. Mater. 196, 1-15. https://doi.org/10.1016/j.jhazmat.2011.08.082.

Bastian M, H. S., Jacomy M., 2009. Gephi: An open source software for exploring and manipulating networks. International AAAI Conference on Weblogs and Social Media. http://www.aaai.org/ocs/index.php/ICWSM/09/paper/view/154.

Bellanger, X.; Guilloteau, H.; Bonot, S.; Merlin, C., 2014. Demonstrating plasmid-

based horizontal gene transfer in complex environmental matrices: A practical approach for a critical review. Sci. Total Environ. 493, 872-882. https://doi.org/10.1016/j.scitotenv.2014.06.070.

Berendonk, T. U.; Manaia, C. M.; Merlin, C.; Fatta-Kassinos, D.; Cytryn, E.; Walsh, F.; Burgmann, H.; Sorum, H.; Norstrom, M.; Pons, M. N.; Kreuzinger, N.; Huovinen, P.; Stefani, S.; Schwartz, T.; Kisand, V.; Baquero, F.; Martinez, J. L., 2015. Tackling antibiotic resistance: the environmental framework. Nat. Rev. Microbiol. 13 (5), 310-317. https://doi.org/10.1038/nrmicro3439.

Blair, J. M.; Webber, M. A.; Baylay, A. J.; Ogbolu, D. O.; Piddock, L. J., 2015. Molecular mechanisms of antibiotic resistance. Nat. Rev. Microbiol. 13 (1), 42-51. https://doi.org/10.1038/nrmicro3380.

Callahan, B. J.; McMurdie, P. J.; Rosen, M. J.; Han, A. W.; Johnson, A. J. A.; Holmes, S. P., 2016. DADA2: High-resolution sample inference from Illumina amplicon data. Nat. Methods 13 (7), 581-583. https://doi.org/10.1038/nmeth.3869.

Chen, Q. L.; Fan, X. T.; Zhu, D.; An, X. L.; Su, J. Q., 2018. Effect of biochar amendment on the alleviation of antibiotic resistance in soil and phyllosphere of Brassica chinensis L. Soil Biol. Biochem. 74-82. https://doi.org/10.1016/j.soilbio.2018.01.015.

Chenu, C., 1993. Clay- or sand-polysaccharide associations as models for the interface between micro-organisms and soil: water related properties and microstructure. Geoderma 56 (1), 143-156. https://doi.org/10.1016/0016-7061(93)90106-U.

Costa, O. Y. A.; Raaijmakers, J. M.; Kuramae, E. E., 2018. Microbial extracellular polymeric substances: Ecological function and impact on soil aggregation. Front. Microbiol. 9, 1636. https://doi.org/10.3389/fmicb.2018.01636.

D'Costa, V. M.; McGrann, K. M.; Hughes, D. W.; Wright, G. D., 2006. Sampling the

antibiotic resistome. Science 311 (5759), 374-377. https://doi.org/10.1126/science.1120800.

Deng, Y.; Li, B.; Zhang, T., 2018. Bacteria that make a meal of sulfonamide antibiotics: blind spots and emerging opportunities. Environ. Sci. Technol. *52* (7), 3854-3868. https://doi.org/10.1021/acs.est.7b06026.

Do, H.; Che, C.; Zhao, Z.; Wang, Y.; Li, M.; Zhang, X.; Zhao, X., 2020. Extracellular polymeric substance from Rahnella sp. LRP3 converts available Cu into $Cu_5(PO_4)_2(OH)_4$ in soil through biomineralization process. Environ. Pollut. 260, 114051. https://doi.org/10.1016/j.envpol.2020.114051.

Gootz, T. D., 2010. The global problem of antibiotic resistance. Crit. Rev. Immunol. 30 (1), 79-93. https://doi.org/10.1615/CritRevImmunol.v30.i1.60.

Hall, M. C.; Mware, N. A.; Gilley, J. E.; Bartelt-Hunt, S. L.; Snow, D. D.; Schmidt, A. M.; Eskridge, K. M.; Li, X., 2020. Influence of setback distance on antibiotics and antibiotic resistance genes in runoff and soil following the land application of swine manure slurry. Environ. Sci. Technol. 54 (8), 4800-4809. https://doi.org/10.1021/acs.est.9b04834.

Hanselman, T. A.; Graetz, D. A.; Wilkie, A. C., 2004. Manure-borne estrogens as potential environmental contaminants: A Review. Environ. Sci. Technol. 37 (24), 5471-5478. https://doi.org/10.1021/es034410+.

Heuer, H.; Schmitt, H.; Smalla, K., 2011. Antibiotic resistance gene spread due to manure application on agricultural fields. Curr. Opin. Microbiol. 14 (3), 236-243. https://doi.org/10.1016/j.mib.2011.04.009.

Hu, X.; Kang, F.; Yang, B.; Zhang, W.; Qin, C.; Gao, Y., 2019. Extracellular polymeric substances acting as a permeable barrier hinder the lateral transfer of antibiotic resistance genes. Front. Microbiol. 10, 736.

https://doi.org/10.3389/fmicb.2019.00736.

Jechalke, S.; Heuer, H.; Siemens, J.; Amelung, W.; Smalla, K., 2014. Fate and effects of veterinary antibiotics in soil. Trends Microbiol. 22 (9), 536-545. https://doi.org/10.1016/j.tim.2014.05.005.

Jia, F.; Yang, Q.; Liu, X.; Li, X.; Li, B.; Zhang, L.; Peng, Y., 2017. Stratification of extracellular polymeric substances (EPS) for aggregated anammox microorganisms. Environ. Sci. Technol. 51 (6), 3260-3268. https://doi.org/10.1021/acs.est.6b05761.

Klindworth, A.; Pruesse, E.; Schweer, T.; Peplies, J.; Quast, C.; Horn, M.; Glöckner, F. O., 2012. Evaluation of general 16S ribosomal RNA gene PCR primers for classical and next-generation sequencing-based diversity studies. Nucleic Acids Res. 41 (1), e1. https://doi.org/10.1093/nar/gks808.

Layeghifard, M.; Hwang, D. M.; Guttman, D. S., 2017. Disentangling interactions in the microbiome: a network perspective. Trends Microbiol. 25 (3), 217-228. https://doi.org/10.1016/j.tim.2016.11.008.

Li, F.; Peng, Y.; Fang, W.; Altermatt, F.; Xie, Y.; Yang, J.; Zhang, X., 2018. Application of environmental DNA metabarcoding for predicting anthropogenic pollution in rivers. Environ. Sci. Technol. 52 (20), 11708-11719. https://doi.org/10.1021/acs.est.8b03869.

Liang, Y.; Pei, M.; Wang, D.; Cao, S.; Xiao, X.; Sun, B., 2017. Improvement of soil ecosystem multifunctionality by dissipating manure-induced antibiotics and resistance genes. Environ. Sci. Technol. 51 (9), 4988-4998. https://doi.org/10.1021/acs.est.7b00693.

Maqbool, T.; Quang, V. L.; Cho, J.; Hur, J., 2016. Characterizing fluorescent dissolved organic matter in a membrane bioreactor via excitation–emission matrix combined

552 with parallel factor analysis. Bioresour. Technol. 209, 31-39.
553 https://doi.org/10.1016/j.biortech.2016.02.089.
554 Muurinen, J.; Stedtfeld, R.; Karkman, A.; Pärnänen, K.; Tiedje, J.; Virta, M., 2017.
555 Influence of manure application on the environmental resistome under finnish
556 agricultural practice with restricted antibiotic use. Environ. Sci. Technol. 51 (11),
557 5989-5999. https://doi.org/10.1021/acs.est.7b00551.
558 Noda, I., 2012. Close-up view on the inner workings of two-dimensional correlation
559 spectroscopy. Vib. Spectrosc. 60, 146-153.
560 https://doi.org/10.1016/j.vibspec.2012.01.006.
561 Noda, I.; Ozaki, Y., 2004. Two-dimensional correlation spectroscopy: Applications in
562 vibrational and optical spectroscopy. John Wiley & Sons, London
563 Oliveira, S. A.; Silva, B. C. d.; Riegel-Vidotti, I. C.; Urbano, A.; Faria-Tischer, P. C. d.
564 S.; Tischer, C. A., 2017. Production and characterization of bacterial cellulose
565 membranes with hyaluronic acid from chicken comb. Int. J. Biol. Macromol. 642-
566 653. https://doi.org/10.1016/j.ijbiomac.2017.01.077
567 Pi, S.; Li, A.; Cui, D.; Su, Z.; Feng, L.; Ma, F.; Yang, J., 2019. Biosorption behavior
568 and mechanism of sulfonamide antibiotics in aqueous solution on extracellular
569 polymeric substances extracted from Klebsiella sp. J1. Bioresour. Technol. 272,
570 346-350. https://doi.org/10.1016/j.biortech.2018.10.054.
571 Quast, C.; Pruesse, E.; Yilmaz, P.; Gerken, J.; Schweer, T.; Yarza, P.; Peplies, J.;
572 Glöckner, F. O., 2012. The SILVA ribosomal RNA gene database project:
573 improved data processing and web-based tools. Nucleic Acids Res. 41 (D1), D590-
574 D596. https://doi.org/10.1093/nar/gks1219.
575 Redmile-Gordon, M. A.; Brookes, P. C.; Evershed, R. P.; Goulding, K. W. T.; Hirsch, P.
576 R., 2014. Measuring the soil-microbial interface: Extraction of extracellular

577 polymeric substances (EPS) from soil biofilms. Soil Biol. Biochem. 72, 163-171.
578 https://doi.org/10.1016/j.soilbio.2014.01.025.
579 Schauss, K.; Focks, A.; Heuer, H.; Kotzerke, A.; Schmitt, H.; Thiele-Bruhn, S.;
580 Smalla, K.; Wilke, B.-M.; Matthies, M.; Amelung, W.; Klasmeier, J.; Schloter, M.,
581 2009. Analysis, fate and effects of the antibiotic sulfadiazine in soil ecosystems.
582 TrAC, Trends Anal. Chem. 28 (5), 612-618.
583 https://doi.org/10.1016/j.trac.2009.02.009.
584 Segata, N.; Izard, J.; Waldron, L.; Gevers, D.; Miropolsky, L.; Garrett, W. S.;
585 Huttenhower, C., 2011. Metagenomic biomarker discovery and explanation.
586 Genome Biol. 12 (6), R60. https://doi.org/10.1186/gb-2011-12-6-r60.
587 Sheng, G. P.; Yu, H. Q.; Li, X. Y., 2010. Extracellular polymeric substances (EPS) of
588 microbial aggregates in biological wastewater treatment systems: A review.
589 Biotechnol. Adv. 28 (6), 882-894.
590 https://doi.org/10.1016/j.biotechadv.2010.08.001.
591 Sher, Y.; Baker, N. R.; Herman, D.; Fossum, C.; Hale, L.; Zhang, X.; Nuccio, E.; Saha,
592 M.; Zhou, J.; Pett-Ridge, J.; Firestone, M., 2020. Microbial extracellular
593 polysaccharide production and aggregate stability controlled by switchgrass
594 (Panicum virgatum) root biomass and soil water potential. Soil Biol. Biochem. 143,
595 107742. https://doi.org/10.1016/j.soilbio.2020.107742.
596 Sköld, O., 2000. Sulfonamide resistance: mechanisms and trends. Drug Resist. Updates
597 3 (3), 155-160. https://doi.org/10.1054/drup.2000.0146.
598 Stedmon, C. A.; Bro, R. J. L.; Methods, O., 2008. Characterizing dissolved organic
599 matter fluorescence with parallel factor analysis: a tutorial. Limnol. Oceanogr.:
600 Methods 6 (11), 572-579. https://doi.org/10.4319/lom.2008.6.572b.
601 Stewart, P. S., 2002. Mechanisms of antibiotic resistance in bacterial biofilms. Int. J.

602 Med. Microbiol. 292 (2), 107-113. https://doi.org/10.1078/1438-4221-00196.
603 Tang, X.; Lou, C.; Wang, S.; Lu, Y.; Liu, M.; Hashmi, M. Z.; Liang, X.; Li, Z.; Liao, Y.;
604 Qin, W.; Fan, F.; Xu, J.; Brookes, P. C., 2015. Effects of long-term manure
605 applications on the occurrence of antibiotics and antibiotic resistance genes (ARGs)
606 in paddy soils: Evidence from four field experiments in south of China. Soil Biol.
607 Biochem. 90, 179-187. https://doi.org/10.1016/j.soilbio.2015.07.027.
608 Udikovic-Kolic, N.; Wichmann, F.; Broderick, N. A.; Handelsman, J., 2014. Bloom of
609 resident antibiotic-resistant bacteria in soil following manure fertilization. Proc.
610 Natl. Acad. Sci. USA 111 (42), 15202-15207.
611 https://doi.org/10.1073/pnas.1409836111.
612 Van Acker, H.; Van Dijck, P.; Coenye, T., 2014. Molecular mechanisms of antimicrobial
613 tolerance and resistance in bacterial and fungal biofilms. Trends Microbiol. 22 (6),
614 326-333. https://doi.org/10.1016/j.tim.2014.02.001.
615 Wang, F.; Xu, M.; Stedtfeld, R. D.; Sheng, H.; Fan, J.; Liu, M.; Chai, B.; Soares de
616 Carvalho, T.; Li, H.; Li, Z.; Hashsham, S. A.; Tiedje, J. M., 2018a. Long-term
617 effect of different fertilization and cropping systems on the soil antibiotic
618 resistome. Environ. Sci. Technol. 52 (22), 13037-13046.
619 https://doi.org/10.1021/acs.est.8b04330.
620 Wang, L.; Li, Y.; Wang, L.; Zhang, H.; Zhu, M.; Zhang, P.; Zhu, X., 2018b. Extracellular
621 polymeric substances affect the responses of multi-species biofilms in the presence
622 of sulfamethizole. Environ. Pollut. 235, 283-292.
623 https://doi.org/10.1016/j.envpol.2017.12.060.
624 Wang, L.; Li, Y.; Wang, L.; Zhu, M.; Zhu, X.; Qian, C.; Li, W., 2018c. Responses of
625 biofilm microorganisms from moving bed biofilm reactor to antibiotics exposure:
626 Protective role of extracellular polymeric substances. Bioresour. Technol. 254,

627 268-277. https://doi.org/10.1016/j.biortech.2018.01.063.
628 Wu, D.; Zhang, Z.; Yu, Z.; Zhu, L., 2018. Optimization of F/M ratio for stability of
629 aerobic granular process via quantitative sludge discharge. Bioresour. Technol.
630 252, 150-156. https://doi.org/10.1016/j.biortech.2017.12.094.
631 Wu, Y.; Cai, P.; Jing, X.; Niu, X.; Ji, D.; Ashry, N. M.; Gao, C.; Huang, Q., 2019. Soil
632 biofilm formation enhances microbial community diversity and metabolic activity.
633 Environ. Int. 132, 105116. https://doi.org/10.1016/j.envint.2019.105116.
634 Xie, W. Y.; McGrath, S. P.; Su, J. Q.; Hirsch, P. R.; Clark, I. M.; Shen, Q.; Zhu, Y. G.;
635 Zhao, F. J., 2016. Long-term impact of field applications of sewage sludge on soil
636 antibiotic resistome. Environ. Sci. Technol. 50 (23), 12602-12611.
637 https://doi.org/10.1021/acs.est.6b02138.
638 Xu, J.; Sheng, G. P., 2020. Microbial extracellular polymeric substances (EPS) acted as
639 a potential reservoir in responding to high concentrations of sulfonamides shocks
640 during biological wastewater treatment. Bioresour. Technol. 123654.
641 https://doi.org/10.1016/j.biortech.2020.123654.
642 Xu, J.; Sheng, G. P.; Ma, Y.; Wang, L. F.; Yu, H. Q., 2013. Roles of extracellular
643 polymeric substances (EPS) in the migration and removal of sulfamethazine in
644 activated sludge system. Water Res. 47 (14), 5298-5306.
645 https://doi.org/10.1016/j.watres.2013.06.009.
646 Yin, C.; Meng, F.; Chen, G. H., 2015. Spectroscopic characterization of extracellular
647 polymeric substances from a mixed culture dominated by ammonia-oxidizing
648 bacteria. Water Res. 68, 740-749. https://doi.org/10.1016/j.watres.2014.10.046.
649 Zhang, D.; Trzcinski, A. P.; Kunacheva, C.; Stuckey, D. C.; Liu, Y.; Tan, S. K.; Ng, W.
650 J., 2016. Characterization of soluble microbial products (SMPs) in a membrane
651 bioreactor (MBR) treating synthetic wastewater containing pharmaceutical

652 compounds. Water Res. 102, 594-606.
653 https://doi.org/10.1016/j.watres.2016.06.059.
654 Zhang, H.; Jia, Y.; Khanal, S. K.; Lu, H.; Fang, H.; Zhao, Q., 2018. Understanding the
655 role of extracellular polymeric substances on ciprofloxacin adsorption in aerobic
656 sludge, anaerobic sludge, and sulfate-reducing bacteria sludge systems. Environ.
657 Sci. Technol. 52 (11), 6476-6486. https://doi.org/10.1021/acs.est.8b00568.
658 Zhang, H.; Song, S.; Jia, Y.; Wu, D.; Lu, H., 2019. Stress-responses of activated sludge
659 and anaerobic sulfate-reducing bacteria sludge under long-term ciprofloxacin
660 exposure. Water Res. 164, 114964. https://doi.org/10.1016/j.watres.2019.114964.
661 Zhang, X.; Fan, W. Y.; Yao, M. C.; Yang, C. W.; Sheng, G. P., 2020. Redox state of
662 microbial extracellular polymeric substances regulates reduction of selenite to
663 elemental selenium accompanying with enhancing microbial detoxification in
664 aquatic environments. Water Res. 172, 115538.
665 https://doi.org/10.1016/j.watres.2020.115538.
666 Zhu, L.; Qi, H. Y.; Lv, M. L.; Kong, Y.; Yu, Y. W.; Xu, X. Y., 2012. Component analysis
667 of extracellular polymeric substances (EPS) during aerobic sludge granulation
668 using FTIR and 3D-EEM technologies. Bioresour. Technol. 124, 455-459.
669 https://doi.org/10.1016/j.biortech.2012.08.059.
670 Zhu, L.; Zhou, J.; Lv, M.; Yu, H.; Zhao, H.; Xu, X., 2015. Specific component
671 comparison of extracellular polymeric substances (EPS) in flocs and granular
672 sludge using EEM and SDS-PAGE. Chemosphere 121, 26-32.
673 https://doi.org/10.1016/j.chemosphere.2014.10.053.
674 Zhu, Y. G.; Johnson, T. A.; Su, J. Q.; Qiao, M.; Guo, G. X.; Stedtfeld, R. D.;
675 Hashsham, S. A.; Tiedje, J. M., 2013. Diverse and abundant antibiotic resistance
676 genes in Chinese swine farms. Proc. Natl. Acad. Sci. USA 110 (9), 3435-3440.

https://doi.org/10.1073/pnas.1222743110.

Figure Captions

Figure 1. Comparison of bacterial communities between bamboo forest soil and farmland soil with a gradient of SDZ addition in the manure. (a) alpha diversity estimated by Shannon index (b) PCoA plot of bacterial community composition based on Bray-Curtis metric distance (c) taxonomic compositions of bacterial communities and cladogram generated by LEfSe indicating difference of taxa induced by the addition of SDZ in bacterial community of bamboo forest soil (d) and farmland soil (e).

Figure 2. The bacterial co-occurrence networks under SDZ presence (Low, Moderate and High) in the manure based on correlation analysis. A node stands for an ASV and a connection represents a strong Spearman's correlation with $p > 0.8$ and significant at p value < 0.01. The bacterial modules (Score > 3) in the networks were clusters of closely interconnected nodes. The nodes of the SDZ presence networks are colored by phyla (a, c) and modules (b, d) respectively for two soils and the size of each is proportional to the number of connections (degree). The red edges represent positive interactions between two ASVs, while the blue stand for negative interactions.

Figure 3. Characterization of EPS expressed using general spectroscopic observations. (a) The amount of EPS represented by DOC concentration (b) FTIR spectra of EPS extracted from two soils and synchronous and asynchronous 2D correlation maps generated from FTIR spectrum of EPS obtained from (c) bamboo forest soil and (d) farmland soil.

Figure 4. Fluorescence components information identified by PARAFAC analysis (a)

699 the spectral shapes and (b) relative amount of two components obtained using
700 fluorescence maximum and the number of replicates for each treatment was eight.
701 Figure 5. The (a) absolute abundance (copies g^{-1}) and (b) relative abundance (gene
702 copies 16S $rRNA^{-1}$) of ARGs in soil. Error bars indicated the standard deviation and
703 different lowercase letters indicated significant difference ($p < 0.05$).
704 Figure 6. Schematic diagram of protective mechanisms potentially occurred in the
705 extracellular and intercellular space of bamboo forest soil (a, b) and farmland soil (c, d)
706 in the presence of low and high concentration.

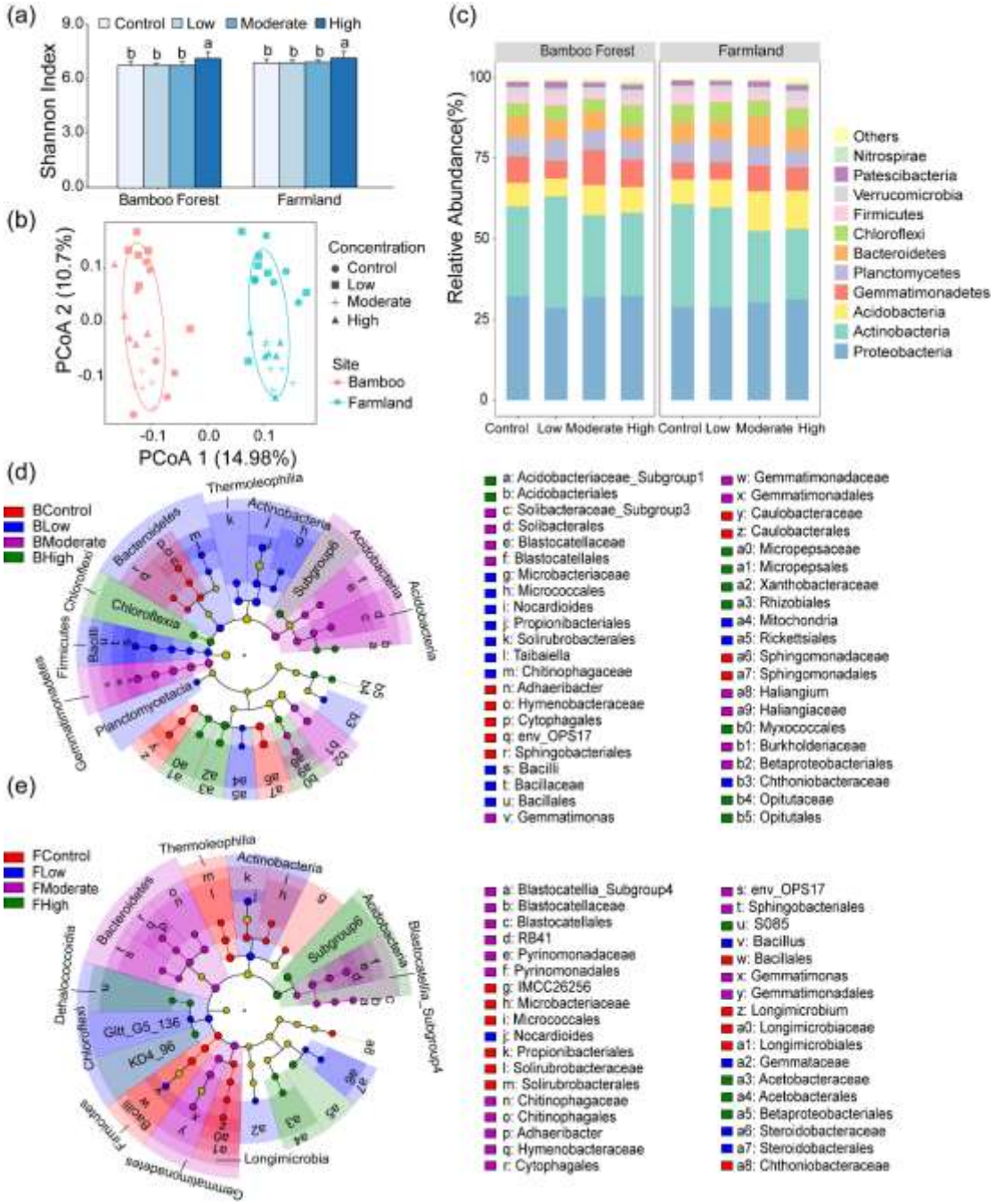
(a)
Control
Low
Moderate
High
Shannon Index
Bamboo Forest
Farmland
(b)
PCoA 2 (10.7%)
PCoA 1 (14.98%)
Concentration
Control
Low
Moderate
High
Site
Bamboo
Farmland
(c)
Bamboo Forest
Farmland
Relative Abundance(%)
Control Low Moderate High Control Low Moderate High
Others
Nitrospirae
Patescibacteria
Verrucomicrobia
Firmicutes
Chloroflexi
Bacteroidetes
Planctomycetes
Gemmatimonadetes
Acidobacteria
Actinobacteria
Proteobacteria
(d)
BControl
BLow
BModerate
BHigh
Thermoleophilia
Actinobacteria
Acidobacteria
Subgroup6
Bacteroidetes
Chloroflexia
Bacilli
Firmicutes
Planctomycetacia
Gemmatimonadetes
a: Acidobacteriaceae_Subgroup1
b: Acidobacteriales
c: Solibacteraceae_Subgroup3
d: Solibacterales
e: Blastocatellaceae
f: Blastocatellales
g: Microbacteriaceae
h: Micrococcales
i: Nocardioides
j: Propionibacteriales
k: Solirubrobacterales
l: Taibaiella
m: Chitinophagaceae
n: Adhaeribacter
o: Hymenobacteraceae
p: Cytophagales
q: env_OPS17
r: Sphingobacteriales
s: Bacilli
t: Bacillaceae
u: Bacillales
v: Gemmatimonas
w: Gemmatimonadaceae
x: Gemmatimonadales
y: Caulobacteraceae
z: Caulobacterales
a0: Micropepsaceae
a1: Micropepsales
a2: Xanthobacteraceae
a3: Rhizobiales
a4: Mitochondria
a5: Rickettsiales
a6: Sphingomonadaceae
a7: Sphingomonadales
a8: Haliangium
a9: Haliangiaceae
b0: Myxococcales
b1: Burkholderiaceae
b2: Betaproteobacteriales
b3: Chthoniobacteraceae
b4: Opitutaceae
b5: Opitutales
(e)
FControl
FLow
FModerate
FHigh
Thermoleophilia
Actinobacteria
Acidobacteria
Subgroup6
Bacteroidetes
Dehalococcoidia
Chloroflexi
Gitt_GS_136
KD4_96
Bacilli
Firmicutes
Gemmatimonadetes
Longimicrobia
Blastocatellia_Subgroup4
a: Blastocatellia_Subgroup4
b: Blastocatellaceae
c: Blastocatellales
d: RB41
e: Pyrinomonadaceae
f: Pyrinomonadales
g: IMCC26256
h: Microbacteriaceae
i: Micrococcales
j: Nocardioides
k: Propionibacteriales
l: Solirubrobacteraceae
m: Solirubrobacterales
n: Chitinophagaceae
o: Chitinophagales
p: Adhaeribacter
q: Hymenobacteraceae
r: Cytophagales
s: env_OPS17
t: Sphingobacteriales
u: S085
v: Bacillus
w: Bacillales
x: Gemmatimonas
y: Gemmatimonadales
z: Longimicrobium
a0: Longimicrobiaceae
a1: Longimicrobiales
a2: Gemmataceae
a3: Acetobacteraceae
a4: Acetobacterales
a5: Betaproteobacteriales
a6: Steroidobacteraceae
a7: Steroidobacterales
a8: Chthoniobacteraceae

Figure 1.

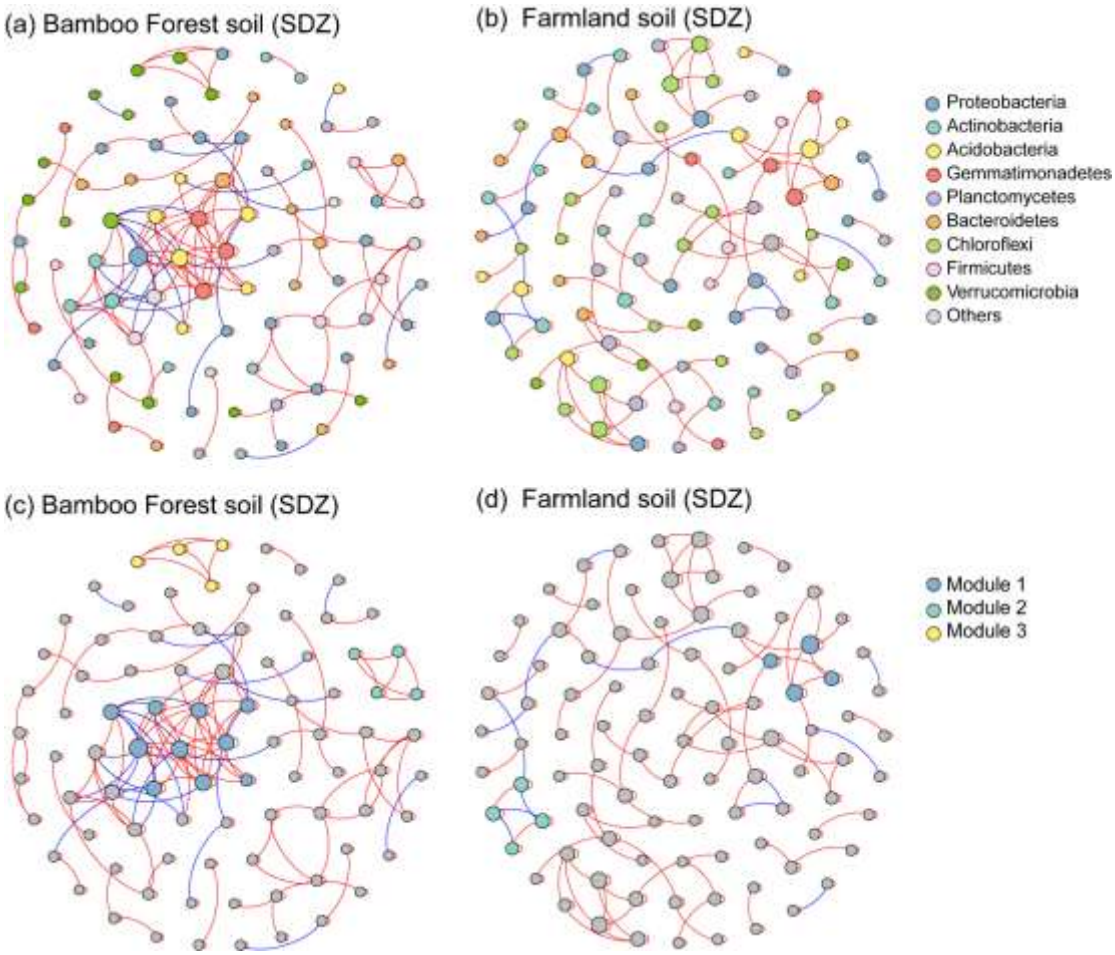
(a) Bamboo Forest soil (SDZ)
(b) Farmland soil (SDZ)
Proteobacteria
Actinobacteria
Acidobacteria
Gemmatimonadetes
Planctomycetes
Bacteroidetes
Chloroflexi
Firmicutes
Verrucomicrobia
Others
(c) Bamboo Forest soil (SDZ)
(d) Farmland soil (SDZ)
Module 1
Module 2
Module 3

Figure 2.

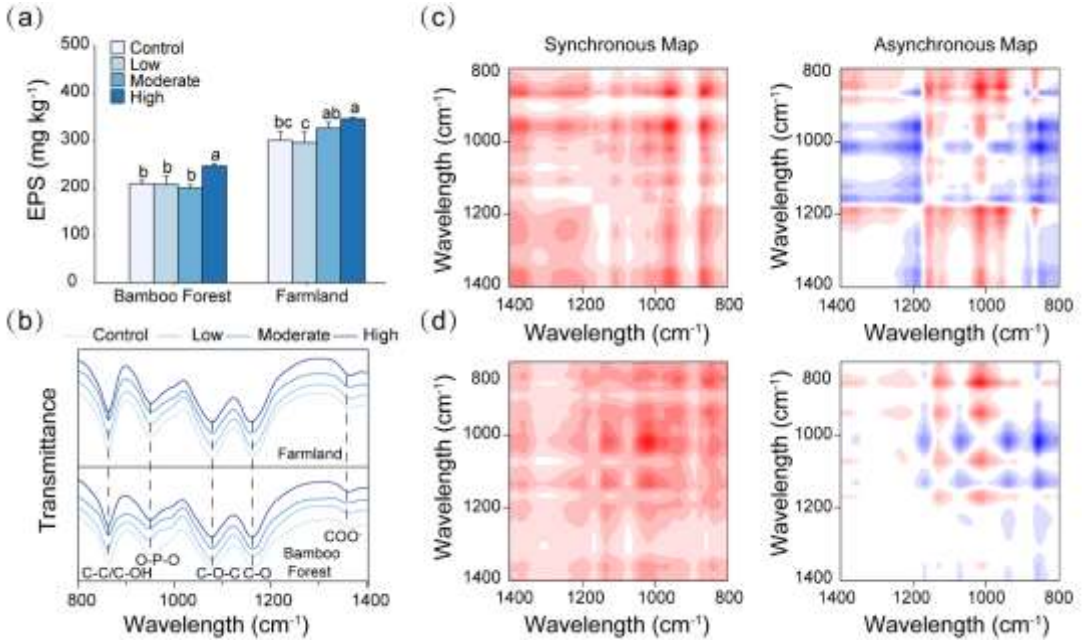
(a)
Control
Low
Moderate
High
EPS (mg kg-1)
500
400
300
200
100
0
b
b
b
a
bc
c
ab
a
Bamboo Forest
Farmland
(b)
Control
Low
Moderate
High
Transmittance
Farmland
Bamboo Forest
C-C/C-OH
O-P-O
C-O-C
C-O
COO-
800
1000
1200
1400
Wavelength (cm-1)
(c)
Synchronous Map
Asynchronous Map
Wavelength (cm-1)
(d)

Figure 3.

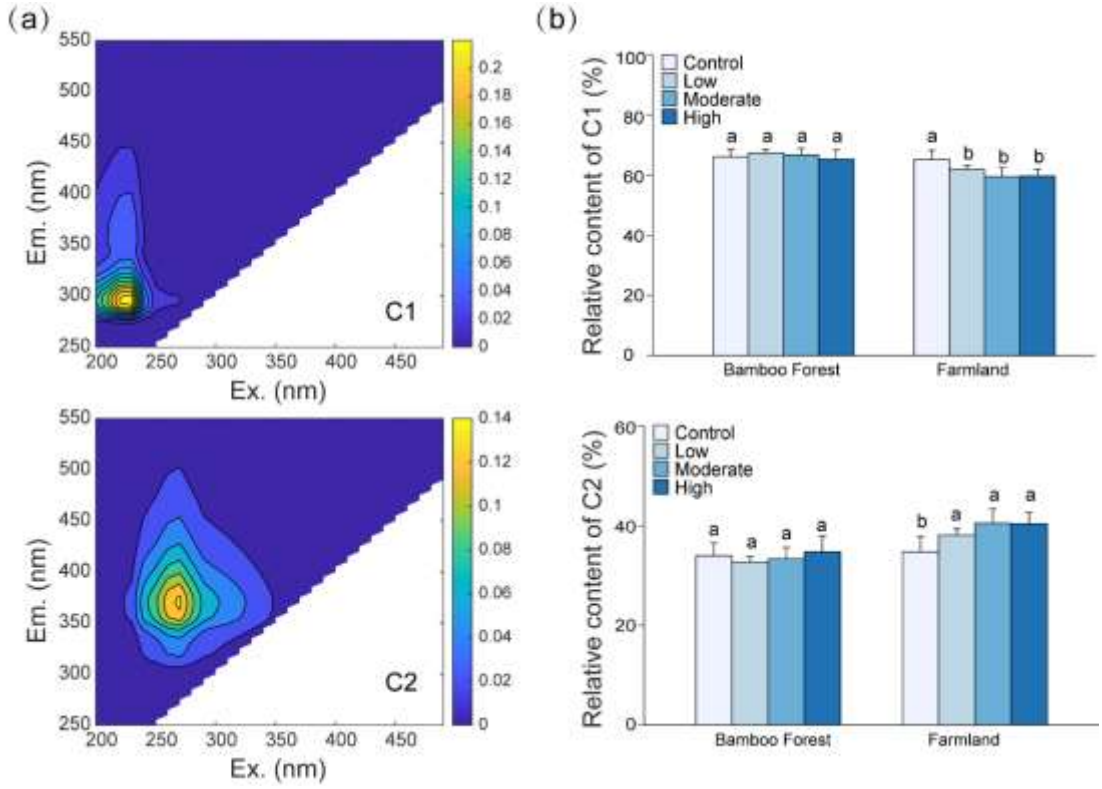
(a)
C1
C2
Em. (nm)
Ex. (nm)
(b)
Control
Low
Moderate
High
Relative content of C1 (%)
Relative content of C2 (%)
Bamboo Forest
Farmland

Figure 4.

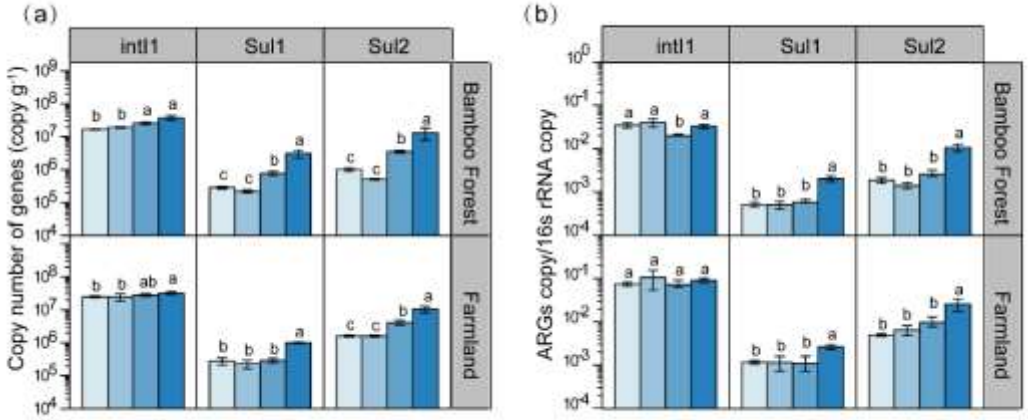
(a)
intI1
Sul1
Sul2
Bamboo Forest
Farmland
Copy number of genes (copy g-1)
(b)
ARGs copy/16s rRNA copy

Figure 5.

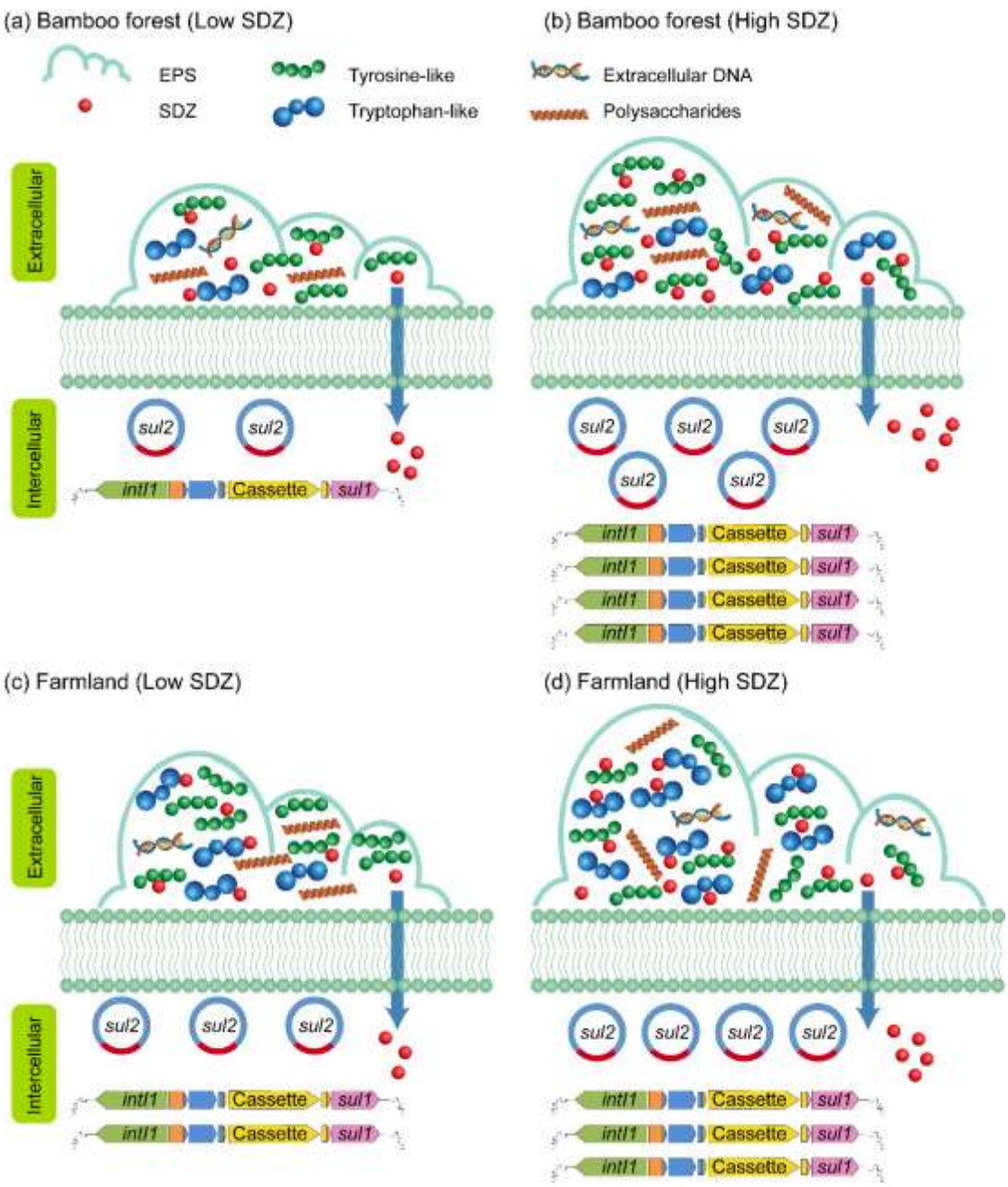
(a) Bamboo forest (Low SDZ)
EPS
SDZ
Tyrosine-like
Tryptophan-like
Extracellular
Intercellular
sul2
intI1
Cassette
sul1
(b) Bamboo forest (High SDZ)
Extracellular DNA
Polysaccharides
(c) Farmland (Low SDZ)
(d) Farmland (High SDZ)

Figure 6.